Simulation of Fast Reactions in Batch Reactors Under Sub-Critical Water Condition

Wael Abdelmoez and Hiroyuki Yoshida
Dept. of Chemical Engineering, Osaka Prefecture University, Osaka 599–8531, Japan

DOI 10.1002/aic.10970
Published online September 1, 2006 in Wiley InterScience (www.interscience.wiley.com).

In this study the temperature profiles inside a tube batch reactor under the sub-critical water condition were investigated under different operating conditions. The most important parameters that may affect the temperature profile, including salt bath mixing speed, reactor shaking, reactant viscosity, and reactor contents, were investigated both experimentally and theoretically. The results showed that both salt bath mixing and reactor shaking had a great effect in the rate of heating up. The study of the effect of reactant viscosity on the temperature profile revealed that the thermal conductivity rather than viscosity was found to affect the temperature profile in the case of comparing reactant with different viscosities. The reactant contents had the lowest pronounced effect on both heating up and cooling down rates among all tested parameters. Two different empirical equations were developed to describe the temperature profiles during both heating up and cooling down periods. Using these equations we developed a new mathematical model for describing the kinetic behavior of fast reactions that take place under the sub-critical water condition. We assumed that the reaction was taking place under unsteady state conditions and following first order kinetics. Based on the simulation results, we developed a new strategy for finding out the correct values of activation energy and frequency factor involved in such fast reactions. © 2006 American Institute of Chemical Engineers *AIChE J,* 52: 3600–3611, 2006

Keywords: reaction kinetics, modeling and simulation, sub-critical water, fast reaction, batch reactor

Introduction

Water is a naturally occurring and abundant substance that exists in solid, liquid, and gas forms on our planet. The physics and chemistry of water are the backbone of engineering and sciences. The characteristics of water at ambient temperature differ completely from those at high temperature and pressure. The water in the vicinity of the critical point is a compressible fluid and, in addition, most of its properties are different in its physics and chemical features. The key properties of water that influence many of the most important interactions are the ion product (the product of the hydrogen ion concentration and the hydroxyl ion concentration) and the dielectric constant (which reflects the polarity and solvent ability of water). Increasing the ion product value increases the hydrogen ion concentration. Therefore, under high ion product values, water possesses the effect of an acid catalyst.[1] On the contrary, the decrease of the dielectric constant decreases the water polarity and allows the dissolving of non-polar compounds in water. Both the ion product and dielectric constant of water can be controlled through controlling the temperature and pressure of the water.[2,3] On heating beyond the critical point of water (temperature $>$ 374°C, pressure $>$ 22.1 MPa), it becomes extremely active and corrosive (supercritical water). However, with temperature control within the critical temperature and under enough pressure to maintain the liquid state (sub-critical water), water can perform very selective extraction processes.[4-6]

Such mild conditions of sub-critical water have attracted

Correspondence concerning this article should be addressed to H. Yoshida at yoshida@chemeng.osakafu-u.ac.jp.

many researchers. Different organic pollutants and waste have been treated utilizing sub-critical water, including decomposition of hazardous organic material,[7] municipal sewage sludge,[8] and marine waste.[6] Earlier work by Yoshida and coworkers showed that a relatively large amount of oil, organic acids, and amino acids could be extracted from fish, squid entrails meat, and cow meat and bone meal wastes using sub-critical water technology.[9-14] Moreover, many useful products were extracted from wood wastes, such as construction scraps and thinning materials, using sub-critical water technology.[15] Recently, the present authors reported a mini review on the different applications of sub-critical water technology in waste reuse, recycling, and treatment.[16]

One of the major problems facing researchers who are dealing with batch reactors under the sub-critical water condition is the correct interpretation of their results. This is particularly important especially in the fast reaction (defined here as the reactions exceeding more than 50% conversion before the stabilization of the temperature inside the reactor) that is taking place during the heating up period while the temperature inside the reactor is continuously changing. The kinetics of such fast reactions are very difficult to track, since the reaction rate tends to follow an Arrhenius behavior, which causes substantial change in the reaction rate with change in temperature. Furthermore, the yields of these reactions are very sensitive to the temperature applied. Thus, it is very important to analyze the kinetic behavior of such fast reactions in batch reactors under the unsteady state condition to get more understanding of the kinetics of these reactions. As an example, the yields of many thermal biomass conversion reactions under the sub-critical water condition are very sensitive to the temperature applied.[17-22] Yet, in some cases, it was possible to overcome this problem by using a flow continuous reactor in which a residence time as less than one second could be achieved using such a system.[19] However, in other cases, it would be impossible to use the laboratory scale flow system under the sub-critical water condition. One such case was in our previous work.[23]

In that work we succeeded in synthesizing a novel protein-based plastic from the bovine serum albumin (a water-soluble protein present in the blood) using sub-critical water technology without the need of any additional catalyst or initiating agents in batch reactors. The optimum synthesis conditions under the sub-critical water condition were found to be in the range of 523-548 K within a reaction time of 0.5-1 minute. During the synthesis period, the temperature inside the batch reactor was continuously increasing with time and, therefore, the synthesis was taking place under unsteady state conditions. It was not possible to follow the synthesis reaction using a laboratory continuous flow reactor type because of the plugging of the rector tubes that resulted from the rapid formation of strong water-insoluble aggregates. This hindered the flow of both reactants and product. Accordingly, we had to find a way to analyze such reactions in a batch reactor under unsteady state conditions.

Accordingly, we explored the literature to find a convenient way to analyze such a very fast reaction or other similar reactions. However, according to the authors' knowledge, this topic has not been addressed previously in a detailed study. We could find only one research that addressed the heat transfer involved in a tube batch reactor.[24] In that work, the heat transfer for batch tubes was analyzed to drive temperature profiles for different tube diameter and evaluate the impact on the biomass conversion. Although they did a very good job, their work was completely based on a theoretical approach without real experimental measurement for the temperature profiles under the actual sub-critical water condition. Moreover, they considered only the effect of the heating up period on the reaction kinetics while neglecting other periods (such as the cooling down period) that could affect the conversion during the course of the reaction, especially at a very fast reaction as the one addressed in our previous work.[23] Therefore, the present work provides a comprehensive analysis of the temperature profile of a tube batch reactor under different sub-critical water conditions both theoretically and experimentally. Moreover, a complete analysis for the kinetic behavior of a modeled fast reaction assuming a first order kinetic is presented as well.

It is important to note that the present work affords the first step in clarifying the kinetics of the synthesis reaction of our novel protein-based plastic synthesized previously,[23] while providing theoretical bases for studying other similar fast reactions using tube batch reactors under sub-critical water conditions or even classical atmospheric conditions.

Materials and Methods

Measuring the temperature profile inside the reactor

The reactor configuration and set up used in this study are shown in Figure 1. The experiments were carried out using a stainless steel pipe SUS 316, i.d. 0.0075 m $\times$ 0.15 m (with a reactor volume of 9.0×10^{-6} m^3) with Swadgelok caps. The reactant was mixed with Milli-Q water and charged into the reactor tube. By applying material balance principles on the three different existing components in the reactor (solid, in the case of a solid sample, liquid, and vapor), the amount of water was calculated to drive the pressure inside the reactor to the saturated water vapor pressure at any given temperature. The values of the saturated vapor pressure at different temperatures were obtained from a steam table. Accordingly, we charged the reactor with a fixed amount of water of 2.5×10^{-6} m^3 throughout all experiments at any given temperature to get good comparable results. Then, dissolved air in the space of the reactor and oxygen in liquid phase were removed by purging argon gas. The tube reactor was then sealed and submerged into a hot salt bath held at a set temperature (Thomas Kagaku Co. Ltd.) containing a mixture of potassium nitrate and sodium nitrate (1:1). The reactions were carried out in the range of 473-573 K at a constant salt bath mixing speed of 210 rpm without shaking (unless stated otherwise). The temperature inside the reactor was measured instantaneously using a thermocouple, φ 3mm with 90% response time of 1.9 sec in water (SC series, CHINO Co., Tokyo, Japan), installed inside the reactor and connected to a digital thermometer having a monitor showing the instantaneous change in the temperature (SUSIO2–01D, CHINO Co., Tokyo, Japan). Using a digital camera, we were able to record the change in temperature with snapshots of the recording monitor. Later, data were collected by viewing the slow-speed film. After reaching a steady state temperature (equal to the bath temperature), the reactor was cooled down by immersion into a water bath. The decrease in the temperature inside the reactor was recorded in the same

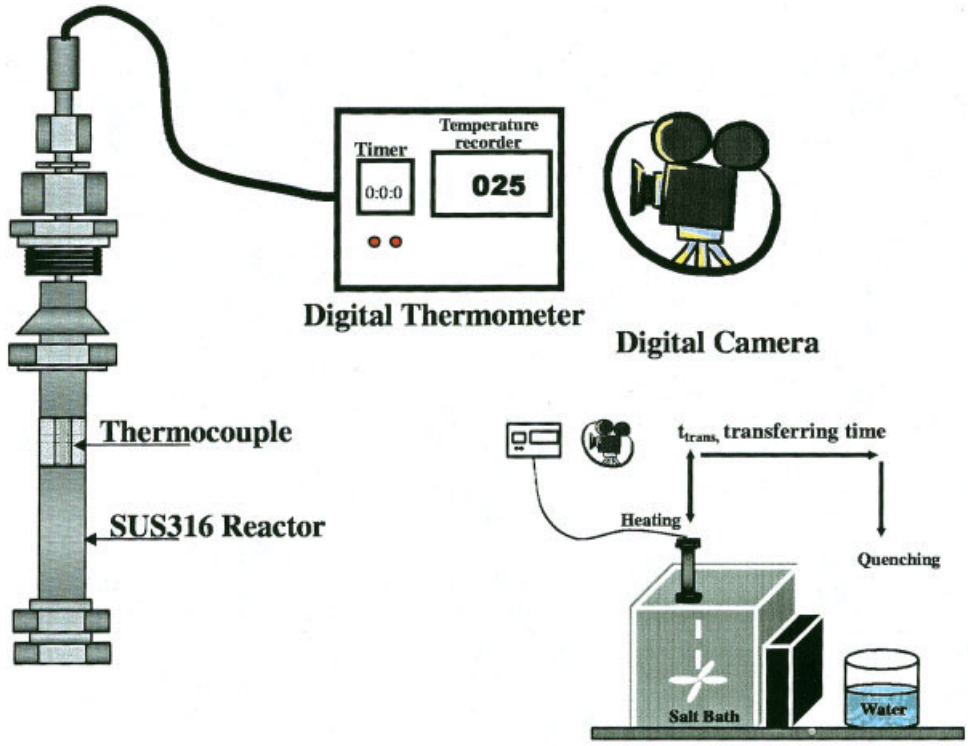

Figure 1. The reactor configuration and setup used for measuring the temperature profile inside the tube batch reactor under the sub-critical water technology.

[Color figure can be viewed in the online issue, which is available at www.interscience.wiley.com.]

way, using the digital camera. All experiments were carried out in triple and presented together.

Parameters affecting the temperature profile inside the reactor

In this study the most important parameters affecting the temperature profile inside the reactor were investigated both theoretically and experimentally. The same procedures described above for measuring the temperature profile were followed in each case, changing only one of the operating parameters. Table 1 summarizes the tested parameters, including the parameter ranges.

Theory

Reactor system

Prior to the beginning of the kinetic study, it was necessary to explore the temperature profile inside the batch reactor used under the sub-critical water condition. Generally, batch reactors are characterized by heating up and cooling down periods. During the heating up period the temperature increases continuously with an increase in the reaction rate and vice versa for the cooling down period. Because the reaction took place in a short time under the unsteady state condition, we had first to figure out equations that could describe the temperature profile

Table 1. The Tested Operating Parameters that Affect the Temperature Profile Inside the Reactor

Parameter	Tested Range	Conditions
Reaction temperature	473–573 K	Only the salt bath temperatures were varied with salt bath mixing of 210 rpm without any reactor shaking.
Mixing speed of the salt bath	0–700 rpm	The salt (in a liquid state) inside the salt bath was mixed at different mixing speed without any reactor shaking at 523 K.
Reactor shaking	0–110 S/min	The reactor was shaken vertically at different shaking speed (expressed as a stroke per minute (s/min)) with salt bath mixing speed of 210 rpm at 523 K.
Reactor contents	0–800 g/L	Different pellets of inert glass (14/16 mesh) were used with different concentrations to study the effect of the reactor contents under salt bath mixing of 210 rpm without any reactor shaking at 523 K.
Reactant viscosity	1.1 and 1499 cp	Pure glycerine with a high viscosity of 1499 cp was used instead of water, which has a low viscosity of 1.1 cP.[25] The experiments were carried out at salt bath mixing speed of 210 rpm at 523 K.

inside the reactor during the heating up and cooling down periods.

Unsteady state analysis of the temperature profile inside the batch reactor

The rate of the energy transfer from the hot salt bath to the stainless steel reactor wall and, hence, inside the reactor depends on both surface and internal resistances. Before inserting the reactor into the hot salt bath ($t \leq 0$), its temperature is equal to the ambient surrounding temperature (298 K). Since the temperature profiles inside the reactor depend on many variables under the sub-critical water condition (for which no specific data are available for accurate mathematical derivation), it was very difficult to develop a derived equation to describe the temperature profiles inside the reactor during both cases of heating up and cooling down. Accordingly, two empirical equations were used based on the data obtained experimentally from measuring the variation of temperature during both heating up and cooling down periods.

For heating up and cooling down periods, Eqs. 1 and 2 were used to calculate the temperature inside the rector during the heating up (T_h) and cooling down (T_c), respectively. These equations were found to fit the experimental data with a considerably high accuracy (as will be shown subsequently in the results and discussion section).

$$T_h = (T_i - T_{bath})\exp[-P_h t_h] + T_{bath} \tag{1}$$

$$T_c = (T_{bath} - T_{water})\exp[-P_c t_c] + T_{water} \tag{2}$$

where t_h represents the heating time and t_c the cooling time. Also, T_i, T_{bath}, T_{water}, P_h, and P_c are the initial ambient temperature (K), steady state salt bath temperature (K), the temperature of the cooling water (K), the heating up rate constant (s^{-1}), and the cooling down rate constant (s^{-1}), respectively. Equations 1 and 2 were fitted to the experimental data using a nonlinear regression fitting to obtain the values of the heating up and cooling down rate constants, P_h and P_c, respectively.

Equation 2 can be rearranged to obtain the instant cooling time t_c at any given temperature during the cooling down period as follows:

$$t_c = \{\ln[(T_c - T_{water})/(T_{bath} - T_{water})]\}/(-P_c), \quad \text{where} \quad T_c \neq T_{water} \tag{3}$$

Then, the total cooling time, t_{tc}, required to cool down the reactor from any temperature T attained by the reactor while in the salt bath to the ambient temperature (298 K) can be calculated as:

$$t_{tc} = t_s - t_c \tag{4}$$

where t_s represents the time needed to cool down the temperature inside the reactor from the steady state salt bath temperature T_{bath} to the ambient temperature (298 K), obtainable from the experimental data of the temperature profile measurement during the cooling down period at a specific temperature.

It is also important to note that there is a transferring time, t_{trans}, representing the required time to transfer the reactor from the hot-salt bath to the cold-water, which should be taken into consideration (in our experiment t_{trans} was found to be only 1 sec). Both t_{trans} and t_{tc} should be used to find out the real reaction time, since the reaction is still taking place during the transferring of the reactor to the cold-water bath and also during the cooling process until the temperature decreases to almost the ambient temperature. Accordingly, the real reaction time can be calculated as follows:

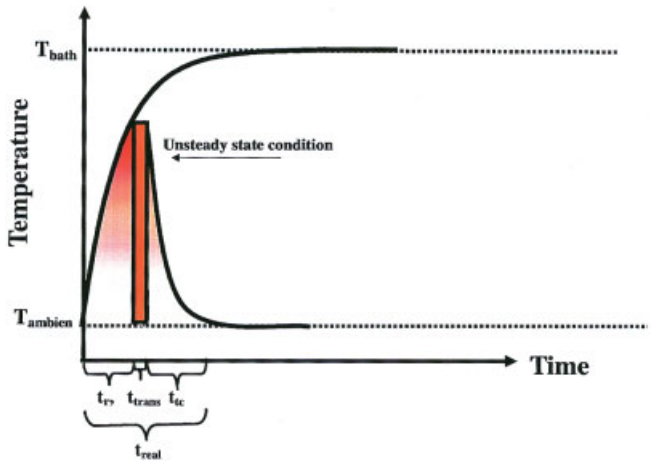

Figure 2. The different reaction stages accompanied by different reaction times existed during fast reactions under the unsteady state condition.

t_r, t_{trans}, t_{tc}, and t_{real} represent the measured reaction time before the quenching step, the time required to transfer the reactor from the hot salt bath to the cooled water, the total time required to cool down the reactor from the temperature T attained by the reactor while in the salt bath to the ambient temperature (298 K), and the real reaction time, respectively. [Color figure can be viewed in the online issue, which is available at www.interscience.wiley.com.]

$$t_{real} = t_r + t_{trans} + t_{tc} \tag{5}$$

where t_{real}, t_r, t_{tc}, and t_{trans} represent the real reaction time, the measured reaction time before the quenching step, the total time required to cool down the reactor from the temperature T attained by the reactor while in the salt bath to the ambient temperature (298 K), and the time required to transfer the reactor from the hot salt bath to the cooled water, respectively. In Eq. 5, t_r and t_{trans} can be measured using a stopwatch during the course of the reaction, and t_{tc} can be calculated for the heating temperature attained by the reactor while in the salt bath from Eqs. 3 and 4.

Figure 2 shows the performance of batch reactors under the unsteady state condition, showing the different reaction times involved during the course of the reaction in the case of the unsteady state condition.

Modeling of the reaction kinetics under the unsteady state condition

In this model we assumed that the reaction scheme could be represented by Eq. 6, which follows a first order kinetic:

$$A \rightarrow B \tag{6}$$

For fast reactions in a tube batch reactor, the reaction is taking place under three different stages, including differing conditions of temperature and time. These stages take place during the heating up period, the transferring of the reactor from the hot salt bath to the cooling bath, and the cooling down stage, respectively. It is of prime importance to understand that the process is carried out under the unsteady state condition in which the temperature is continuously changing.

The conversion rate of the reactant, A, can be represented as follows:

$$-r_A = -dC_A/dt = k(T)C_A \tag{7}$$

where r_A is the conversion rate of A (g/L.s), k(T) represents a function of temperature dependence of the reaction rate constant, and C_A is the concentration of A at any time (g/L).

Assuming that the reaction is temperature-dependent, the Arrhenius equation is given by:

$$k(T) = k_0\text{Exp}[-E/RT(t)] \tag{8}$$

where k_0 is the frequency factor (s^{-1}), E is the activation energy (J/mol), R is the universal gas constant (R = 8.314 J/mol K), T is the reaction temperature (K), and t is the reaction time (s). In Eq. 7, T(t) is the time dependence function of the temperature changing inside the reactor. The function T(t) is represented by Eqs. 1 and 2 for the heating up and cooling down periods, respectively.

Based on the above discussion, we categorized the reaction into three stages. The first stage takes place during the heating up period and is represented by the period from zero time to the reaction time, t_r.. The second stage takes place during the transferring of the reactor from the hot salt bath to the cold water and is represented by the period from t_r to ($t_r + t_{trans}$). The third stage takes place during the cooling down period and is represented by the time from $t_r + t_{trans}$ to t_{real}.

The Reaction During the Heating Up Stage. To obtain the reaction rate during the heating up stage, we substitute Eq. 1 for Eq. 8. It then represents the heating up stage as:

$$-r_{Ah} = -dC_{Ah}/dt = \{k_0\text{Exp}[-(E/R)/[(T_i - T_{bath})\text{exp}[-P_h t_h] + T_{bath}]]\}C_{Ah} \tag{9}$$

where C_{Ah} represents the concentration of A during the heating up stage by rearranging

$$-dC_{Ah}/C_{Ah} = \{k_0\text{Exp}[-(E/R)/[(T_i - T_{bath})\text{exp}[-P_h t_r] + T_{bath}]]\}dt \tag{10}$$

By integrating Eq. 9 we can get the concentration of A during the heating up stage, C_{Ah}:

$$\int_{C_{A0}}^{C_{Ah}} -dC_{Ah}/C_{Ah} = \int_0^{t_r} k_0\text{Exp}[-(E/R)/[(T_i - T_{bath})\text{exp}[[-P_h t_r] + T_{bath}]]dt \tag{11}$$

where C_{A0} is the initial concentration of A. Only the left-hand side of Eq. 11 can be solved analytically, while the right-hand side can be solved numerically. With the integration of the left-hand side, Eq. 11 becomes:

$$-\ln(C_{Ah}/C_{A0}) = \int_0^{t_r} k_0\text{Exp}[-(E/R)/[(T_i - T_{bath})\text{exp}[-P_h t_r] + T_{bath}]]dt \tag{12}$$

where rearranging gives us:

$$C_{Ah} = -C_{A0}\text{Exp}\int_0^{t_r} k_0(\text{Exp}[-(E/R)/[(T_i - T_{bath})\text{exp}[-P_h t_r] + T_{bath}]]dt) \tag{13}$$

From Eq. 13 the concentration of the product, C_{Bh}, which is produced during the heating up stage, can be calculated as:

$$C_{Bh} = C_{A0} - C_{Ah} \tag{14}$$

The Reaction During Transferring The Reactor from the Hot Bath to the Cold Water. During the reactor transferring stage, we assumed that the temperature is constant (since the transferring time, 1 sec, is too short to change the temperature) and equal to the temperature attained at time equal to t_r during the heating up period, calculated from Eq. 1 by substituting t_h for t_r. Then, the temperature during the transfer of the reactor, T_{trans}, could be obtained as follows:

$$T_{trans} = (T_i - T_{bath})\text{exp}[-P_h t_r] + T_{bath} \tag{15}$$

At the transferring stage, the remaining unconverted A during the heating up stage will react to form the new molecules of B. So, the new initial concentration of A that will react during the transferring stage, C_{At0}, can be calculated as:

$$C_{At0} = C_{A0} - C_{Bh} \tag{16}$$

where C_{Bh} represents the concentration of the produced B during the heating up period. The concentration of A during the transferring step C_{At} can be calculated by modifying Eq. 13 as follows:

$$C_{At} = C_{At0}\text{Exp} - \int_{t_r}^{t_{trans}+t_r} k_0(\text{Exp}(-E/RT_{trans})dt) \tag{17}$$

Since the value of ($-E/RT_{trans}$) is constant, the integration of Eq. 17 results in:

$$C_{At} = C_{At0}\text{Exp} - [k_0\text{Exp}(-E/RT_{trans})](t_{trans}) \tag{18}$$

Then, the concentration of the product, C_{Bt}, produced during the transferring stage can be calculated as:

$$C_{Bt} = C_{At0} - C_{At} \quad (19)$$

The Reaction During the Cooling Down Stage. At the quenching step, the remaining unconverted A continued the reaction to form new molecules of B. So, the initial concentration of the A during the cooling down stage, C_{Ac0}, can be calculated as:

$$C_{Ac0} = C_{A0} - C_{Bh} - C_{Bt} \quad (20a)$$

where C_{Bt} represents the concentration of the produced B during the transferring period.

Substituting Eq. 2 for Eq. 8 and rearranging in the same way as previous equations, the concentration of A during the cooling down step, C_{Ac}, can be calculated as:

$$C_{Ac} = -C_{Ac0}\mathrm{Exp}\int_{t_r+t_{trans}}^{t_{real}} k_0(\mathrm{Exp}[-(E/R)/[(T_{bath} - T_{water}) \times \exp[-P_c t_c] + T_{water}]]dt) \quad (20b)$$

Then, the concentration of the product, C_{Bc}, produced during the cooling down stage can be calculated as:

$$C_{Bc} = C_{Ac0} - C_{Ac} \quad (21)$$

Then, the total concentration of the product, C_{BT}, can be calculated by subtracting the summation of C_{Ah} ,C_{At}, and C_{Ac} from the initial concentration of A, C_{A0}:

$$C_{BT} = C_{A0} - (C_{Ah} + C_{At} + C_{Ac}) \quad (22)$$

For a simultaneous calculation of the different concentrations of the product B at different stages, a computer program was developed in this work using the C^{++} programming language. By means of trial and error, the values of E and k_0 should be changed until the calculated concentrations fit the experimental data. More detailed discussion will be given later concerning the criteria of selecting and fine-tuning the values of E and k_0 until they match the correct required values.

Results and Discussion

The first step in this study was to investigate the temperature profile inside the batch reactor while studying the most important parameters that may affect its performance. It is important to note here that all measurements were done under the subcritical water condition using a pressure value that corresponds to the saturated vapor pressure of water at the employed reaction temperature for a rector that is mostly filled by vapor space. Figure 3 shows the temperature profiles inside the reactor at different temperatures in the range of 473-573 K. The experimental data were fitted with Eqs. 1 and 2 for the heating up and cooling down periods, respectively. The results showed that the experimental results were in very good agreement with the theoretical predictions calculated using the empirical equations in the temperature range of 473-548 K. However, the theoretical predication begins to slightly deviate from the experimental data at temperatures higher than 548 K. Accordingly, a significant deviation is expected if these two equations applied to temperatures higher than 573 K especially in the supercritical regime.

The heating up and cooling down rate constants, P_h and P_c, were calculated at different temperatures by fitting the experimental data with Eqs. 1 and 2 using the nonlinear regression method. Table 2 lists the calculated values of P_h and P_c at different temperatures. The results showed that as the reaction temperature increases, both P_h and P_c values increase. However, the rate of cooling down was faster than the rate of heating up at all tested temperatures. These values were calculated based on three repeated experiments carried out under exactly the same conditions. Both P_h and P_c were calculated as an average value of the three experiments. The values of these parameters were used later in the calculation of the kinetic models.

Concerning the parameters that may affect the temperature profile inside the reactor, Table 3 summarizes the values of P_h and P_c calculated under different operating conditions.

Figure 4 shows the effect of the salt bath mixing speed at 523 K on the temperature profile. As we can see, the rate of heating up increases with the increase in the salt bath mixing speed. The values of the heating up rate constant, P_h, were calculated from the experimental data using Eq. 1 to be 0.044, 0.064, 0.084, and 0.12 s^{-1} for a salt bath mixing speed of 0, 210, 350, and 700 rpm, respectively.

Figure 5 shows the combined effect of both reactor shaking and salt bath mixing speed at 523 K. The results show that with no salt bath mixing (0 rpm), as the reactor shaking speed increases, the heating up rate constant increases. The values of P_h were 0.044, 0.1, and 0.13 s^{-1} for shaking speeds of 0, 65, and 110 S/min, respectively. When mixing the salt bath at 700 rpm and shaking the reactor at 115 S/min, the heating up rate constant increased further to reach 0.16 s^{-1}. It was also found that controlling the salt bath mixing speed could be an alternative way to compensate for the effect of the reactor shaking on the temperature profile in situations where it is difficult to shake the reactor. With no reactor shaking at the salt bath mixing speed of 700 rpm, the heating up rate constant was calculated to be 0.12 s^{-1}. This value is very close to the case in which the reactor was shaken at 110 S/min without mixing the salt bath (0.13 s^{-1}). However, the reactor shaking might have another effect on the reaction rate by homogenizing and mixing the reaction media. It is important to note here that shaking and mixing parallel issues in the cooling water bath are expected to reduce the cooling time too, having similar effects as in the case of the hot salt bath. However, in this study, we just showed the effect in the case of the salt bath to reduce the number of the studied parameters and presented data.

Figure 6 shows the effect of the viscosity on the temperature profile. The reactant viscosity only slightly affected the rate of heating up; however, it had a dramatic effect on the rate of cooling down. The results showed that by using a viscous reactant with 1449 cp, the heating up rate constant was reduced by about 21% compared to a reactant viscosity of 1.1 cp (from 0.064 s^{-1} at 1.1 cp to 0.05 s^{-1} at 1449 cp).[25] However, the cooling down rate constant was greatly reduced, by about 72% (from 0.082 s^{-1} at 1.1 cp to 0.023 s^{-1} at 1449 cp). This behavior may be explained on the basis of the effect of temperature not only on the viscosity but specifically in the thermal

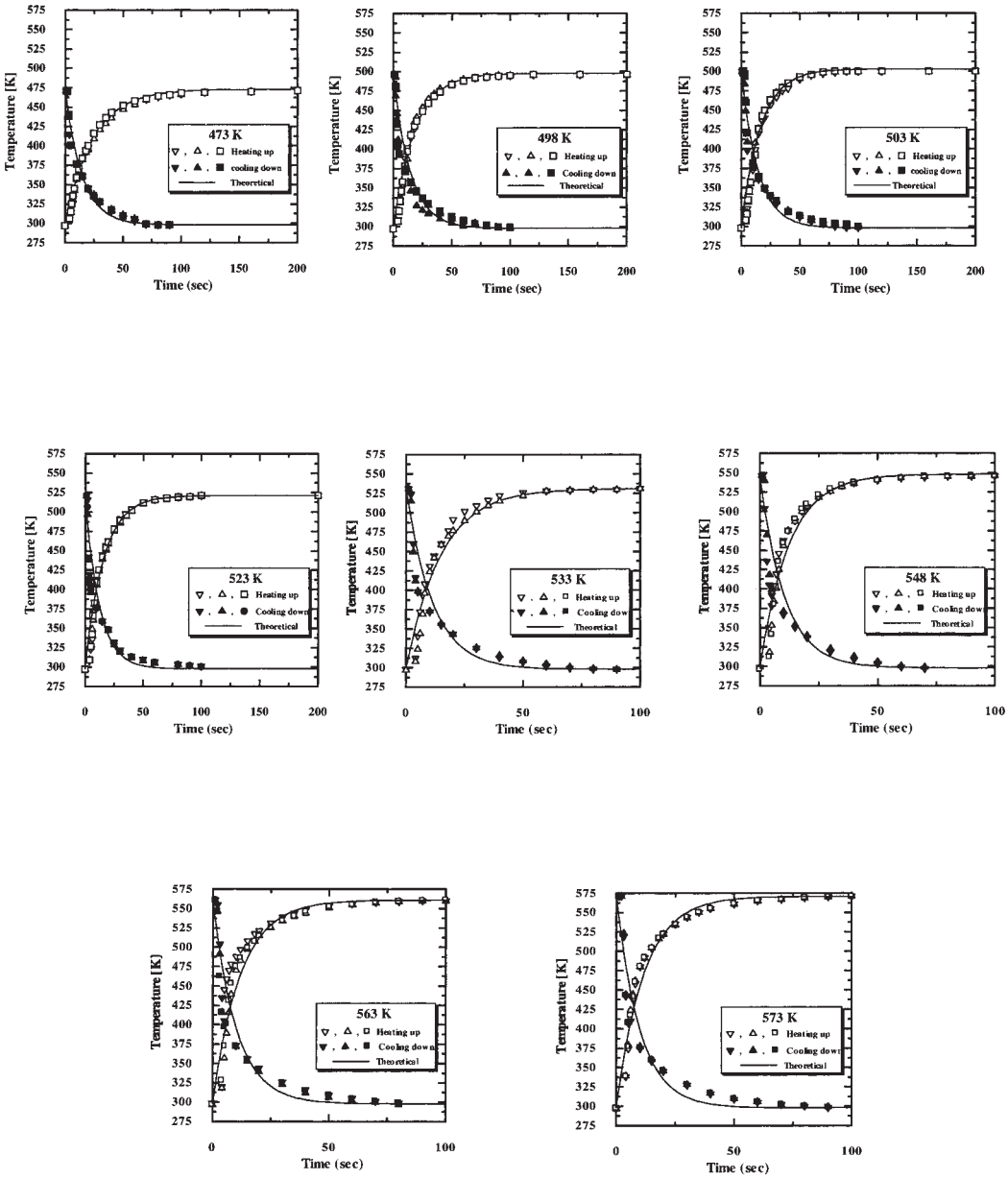

Figure 3. The effect of the salt bath temperature on the temperature profile inside the tube batch reactor under the sub-critical water condition.

conductivity of both glycerine and water under different temperatures.

By looking to the nature of both viscosity and thermal conductivity properties, one can draw a basic understanding of the effect of each property in the temperature profile. Basically, the viscosity is a property that is relevant in fluid flow, while thermal conductivity is the major property affecting the heat conduction. It was reported that heating water from 293 K to 350 K resulted in about 65% reduction in its viscosity (from 1.005 to 0.3565 cP, respectively).[25] Concerning the thermal conductivity, it was reported that the thermal conductivity of water increases upon heating from 293 K to 350 K by about 14% (from 0.00141 to 0.00163 gram cal. cm/cm^2.sec^1. °C^1, respectively).[25] However, the situation in the case of glycerine is quite different.

Heating Dow synthetic glycerine from 293 K to 350 K

Table 2. The Heating Up and Cooling Down Parameters of the Tube Batch Reactor at Different Temperatures

Temp. (K)	473	498	503	523	533	548	563	573
P_h	0.042	0.055	0.061	0.064	0.068	0.082	0.084	0.086
P_c	0.067	0.069	0.070	0.082	0.088	0.095	0.098	0.100

The salt bath mixing speed was 210 rpm without reactor shaking.

Table 3. Summary of the Heating Up and Cooling Down Rate Constants, P_h and P_c, Under Different Operating Conditions at 523 K

No	Salt Mixing Speed (rpm)	Reactor Shaking Speed (S/min)	Viscosity (cP)	Reactor Contents (−)	P_h (s^{-1})	P_c (s^{-1})
1	0.0	0.0	1.1	H_2O	0.044	0.082
2	210	0.0	1.1	H_2O	0.064	0.082
3	350	0.0	1.1	H_2O	0.084	0.082
4	700	0.0	1.1	H_2O	0.120	0.082
5	0.0	65	1.1	H_2O	0.100	0.082
6	0.0	110	1.1	H_2O	0.130	0.082
7	700	115	1.1	H_2O	0.160	0.082
8	210	0.0	1449	Glycerine	0.050	0.023
9	210	0.0	−	Glass beads and H_2O (400 g/L)	0.064	0.085
10	210	0.0	−	Glass beads and H_2O (800 g/L)	0.075	0.085

resulted in about 98% reduction in its viscosity (from 1410 to 31.9 cP, respectively) but at the same time the thermal conductivity did not change (having a constant value of 0.00068 gram cal. $cm/cm^2.sec^1.\ °C^1$ at both tested temperatures). It is now becoming clear that the thermal conductivity of glycerine is lower than that of water by roughly a factor of two in both the heating up and cooling down periods.[25] Accordingly, there will be less conductive heat transfer through the glycerine during both periods when compared to water; therefore, one would expect a longer time to be required to heat up and cool down the glycerine. Moreover, during the cooling down period, the conduction is further reduced due to the stagnant conduction that occurred with the reactor being cooled in the stagnant water bath, which resulted in a great difference between the glycerine and water cooling down rate constants. Therefore, it could be concluded that the thermal conductivity is the major property affecting conduction rather than viscosity and should be the main reason behind the difference in both the heating up and cooling down profiles between water and glycerine.

Figure 7 shows the effect of the reactor contents on the temperature profile. The results indicated that at a solid concentration (represented by the inert glass bead) of 400 g/L, there was a slight effect of reactor contents on the rates of heating up and cooling down. However, at a solid concentration of 800 g/L, the rate of heating up increased without affecting the cooling down rate. Generally, it was found that the reactor contents had the lowest pronounced effect on both heating up and cooling down rates among all tested parameters.

From the above-obtained results concerning the parameters affecting the temperature profile, the following recommendations can be made:

(1) For kinetic and comparative studies, it is very important to operate under the same conditions of salt bath mixing and reactor shaking speeds.

(2) It is very important for reducing the period of the thermal unsteady state condition to operate at a high speed of both salt bath mixing and reactor shaking to increase the heating up rate.

(3) In the case of comparing different reactions with dif-

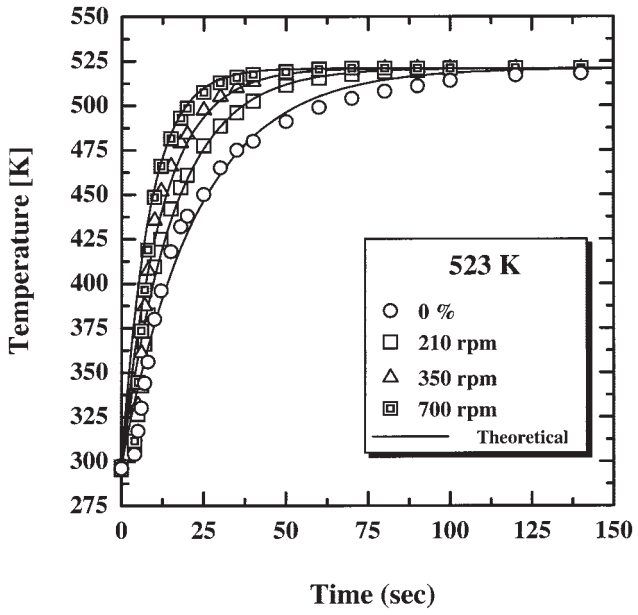

Figure 4. The effect of the salt bath mixing speed on the temperature profile inside the tube batch reactor under the sub-critical water condition.

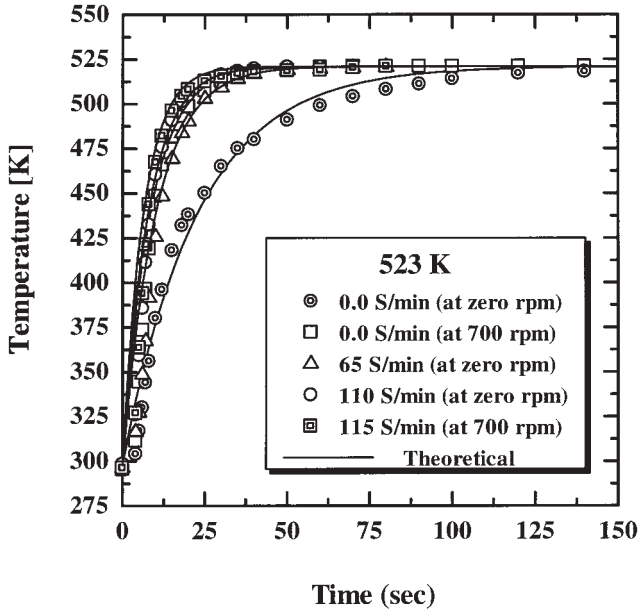

Figure 5. The combined effect of the salt bath mixing speed and reactor shaking on the temperature profile inside the tube batch reactor under the sub-critical water condition.

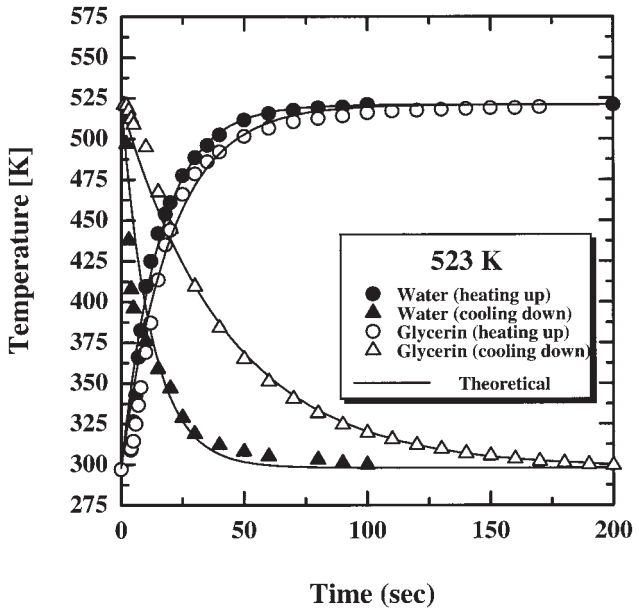

Figure 6. The effect of the reactant viscosity on the temperature profile inside the tube batch reactor under the sub-critical water condition.

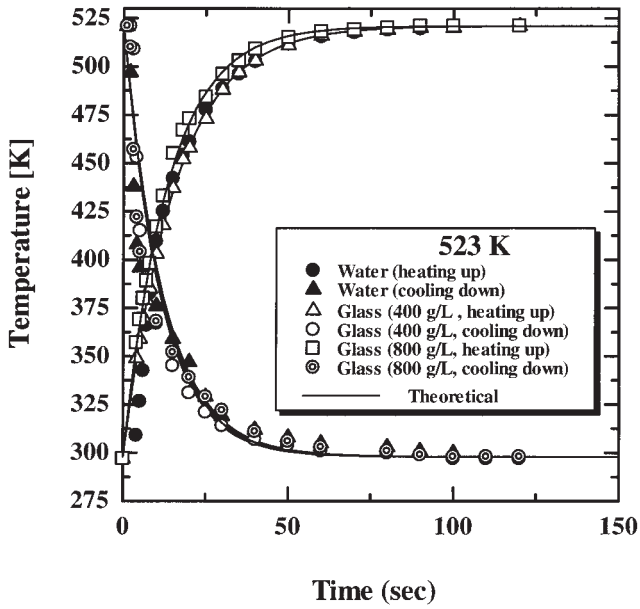

Figure 7. The effect of the reactor contents on the temperature profile inside the tube batch reactor under the sub-critical water condition.

ferent reactant viscosities, the thermal conductivity rather than the viscosity parameter should be considered since it is very important to consider the reduction of the cooling down rate due to the thermal conductivity difference.

(4) There need not be restrictions on working with different reactor contents, since the reactor contents has only a slight effect on the rates of heating up and cooling down.

The second step in this study was to develop a mathematical model for predicting the kinetics of such fast reactions based on the temperature profile study carried out in the first step. The details of the mathematical model were presented and discussed in the theoretical part of this work. According to that model, both activation energy (E) and frequency factor (k_0) represent the main parameters that should be roughly estimated before starting to run the model. Other conditions are also needed to work as boundary conditions to the model. Accordingly, in this work we developed a strategy for selecting the initial values of both E and k_0 as well as setting other conditions.

Based on the experimental data of a kinetic study of a particular reaction, educated guesses should be made to define control borders for the models. As a plan for approaching this goal, we proposed the following strategy:

(1) The values of E and k_0 required to start the trial and error routine could be first evaluated assuming that the reaction is taking place under a steady state condition (following a first order kinetic). Then, values lower than those obtained could be used for the initiation of the trial and error routine.

(2) It is very important to define whether the reaction proceeds during the cooling down period, or it will be stopped due to the interruption resulted from the quenching step. Based on this assumption, the effect of the cooling down reaction on the overall reaction could be eliminated and the reaction will be assumed to proceed during the heating up and transferring steps only.

(3) If the reaction proceeds during the cooling down period, will it proceed at any reaction temperature above the ambient temperature or does it need a certain temperature to initiate the reaction?

Consistent with the above-mentioned strategy, the variation of product concentration versus time was calculated under different conditions and shown in Figures 8-10. All calculations were done assuming a fixed salt bath temperature of 473 K. The measured t_s value at this temperature was found to be 82 sec under the condition that the salt bath mixing speed was 210 rpm without shaking the reactor. The used P_h and P_c values under such conditions were 0.042 and 0.067 s^{-1}, respectively.

At the beginning, to have a clear view about the effect of the different stages of the reaction in the overall concentration profile, we calculated the time of each stage as a function of the reaction time, t_r (the time elapsed for the reactor inside the hot salt bath before the transferring and quenching steps). The

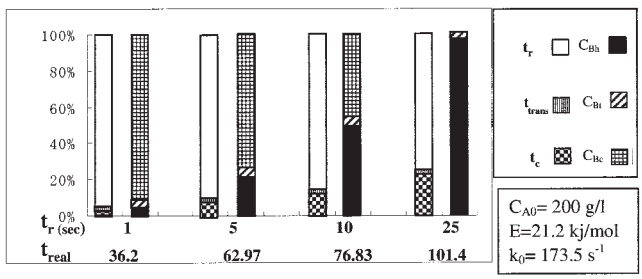

Figure 8. The percentages of the time of the different reaction stages and their relevant product concentration relative to the total real reaction time, t_{real} (t_r + t_{trans} + t_{tc}), and total concentration, C_{BT} (C_{Bh} + C_{Bt} + C_{Bc}), respectively, at 473 K.

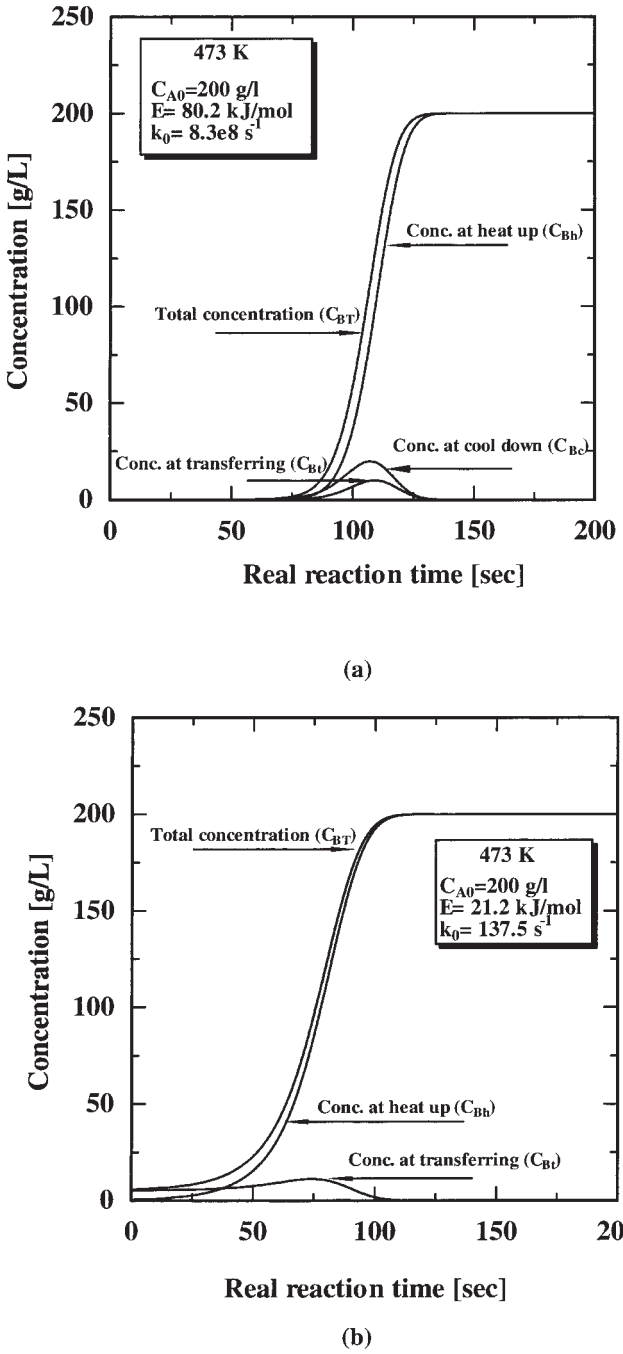

Figure 9. The total concentration of the product B(C_{BT}), the concentration of B produced during the heating up (C_{Bh}), transferring (C_{Bt}), and cooling down (C_{Bc}) stages, against the real reaction time ($t_r + t_{trans} + t_{tc}$) at lower (a) and higher (b) values of E and k_o.

calculations were carried out assuming relatively low values of activation energy and pre-exponential factors (such low values signify a relatively fast reaction, which seemed to be close to our fast reaction case). Figure 8 shows the percentages of the time of the different reaction stages and their relevant product concentration relative to the total real reaction time, t_{real} (t_r + t_{trans} + t_{tc}), and total concentration, C_{BT}, respectively. The calculations were carried out at different t_r values of 1, 5, 10, and 25 sec, considering that the steady state salt bath temperature is kept constant at 473 K. The calculations revealed that at lower t_r values, the time needed for cooling down the reactor, t_{tc}, was very long compared to the t_r and represents more than 94% of the total real reaction time, t_{real}. For t_r value of 1 sec, the value of the real reaction time, $t_{rea,}$ was 36.2 sec, of which

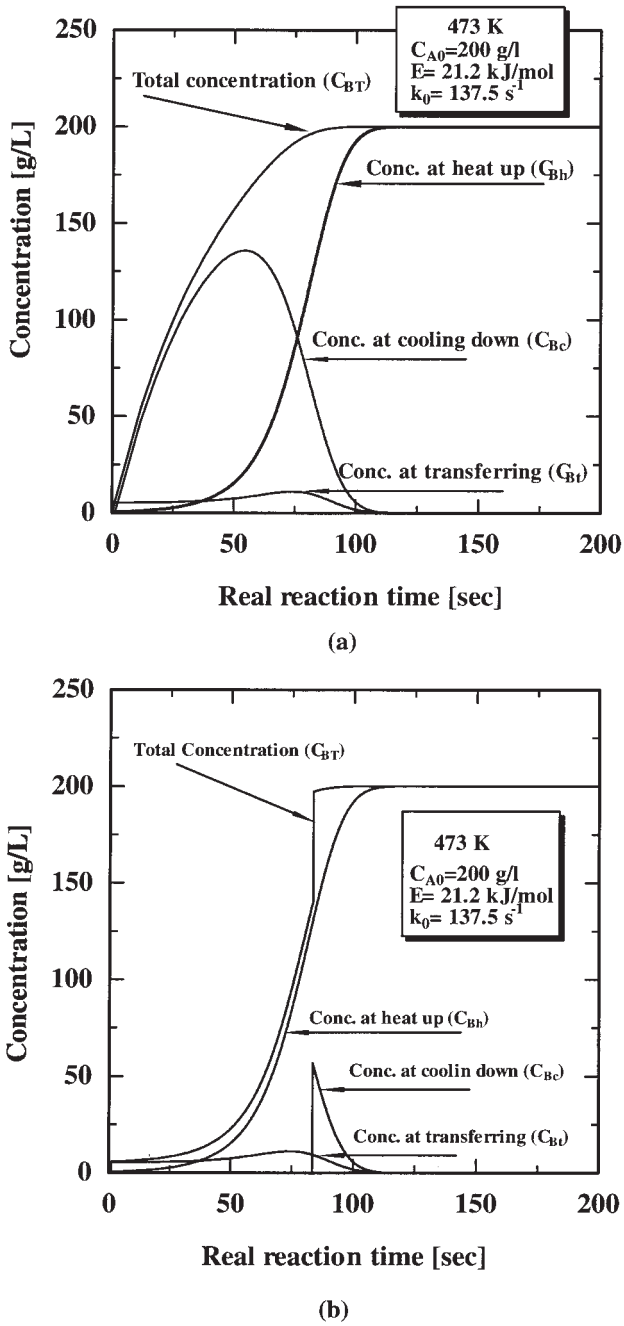

Figure 10. The effect of the cooling down stage on the total concentration of the reaction product under different assumptions.

(a) The cooling down stage was completely neglected, and (b) The cooling down stage proceeds when the heating up temperature reaches 373 K.

the t_{tc} was 34.2 sec and the transferring time was set to be constant at 1 sec at any t_r value (as it was measured experimentally). Accordingly, the concentration of the product B formed during the cooling period represented the highest percentage among other reaction stages. The reason behind such a long t_{tc} value could be explained based on the low driving force available for cooling down the reactor at very short t_r values. Such a driving force originates from the temperature difference between the heating up temperature and ambient temperature, which is very low at lower t_r values. At higher t_r values, the percentage of the product concentration shifted towards the heating up period and minimized during the cooling down period.

Next, to explore the situation more widely, we calculated the total concentration of the product B(C_{BT}), the concentration of B produced during the heating up (C_{Bh}), transferring (C_{Bt}), and cooling down (C_{Bc}) stages, respectively, against the real reaction time (t_{real}) under different conditions of activation energy, E, and frequency factor, k_0, under a wide range of real reaction times (Figure 9). Two different E and k_0 values were used in the calculation. Figure 9a shows the results of using low values of E and k_0 of 21.1 kJ/mole and 137.5 s^{-1}, respectively. However, Figure 9b shows the results of using high values of E and k_0 of 80.2 kJ/mole and 8.3E+08 s^{-1}, respectively. The calculations showed that the product concentration was very high during the cooling down stage over the other reaction stages at low t_{real} values and lower E and k_0 values (lower E and k_0 signify a very fast reaction with relative temperature insensitivity). However, by increasing the t_{real}, the concentration of B during the cooling down and transferring periods increases with lower rate at higher t_{real} values until it reaches a maximum value. After that it decreased very rapidly, with a dramatic increase in the concentration of B during the heating up stage. The explanation of such behavior is quite simple, since at the low t_{real}, which means low t_r in turn, the time allowed for the reaction to react in the heating up period is very short while the time of cooling down is relatively very long (as we showed before in Figure 8). On the other hand, at high t_{real} values, which mean high t_r in turn, the majority of the reactant is exhausted during the heating up stage, resulting in demolishing the effects of both the transferring and cooling down stages.

At higher E and k_0 values (which signify a relatively slow reaction rate with high temperature sensitivity), the reaction rate slows down at low temperatures until the reaction temperature increases to the limit needed to activate the reaction. To approach this relatively high temperature, the reactant needs a longer time for heating up. Accordingly, most of the reactant will be exhausted during the heating up stage, which results in demolishing the effects of the other stages on the overall yield. Therefore, the reaction during the heating up period came to predominate over the other stages.

Now let us address the second option in the developed strategy for finding the E and k_0 values for very fast reactions. Figure 10 shows the effect of the reaction during the cooling down stage on the total concentration of the reaction product. As the simulation showed, if the cooling down stage was completely neglected, the concentration profile changed from being a hyperbolic one (as shown in Figure 9a) to becoming sigmoidal (as shown in Figure 10a). Such behavior could be a clue for detecting the proceeding of the reaction during the cooling down stage. When the simulation was carried out under the assumption that the cooling down reaction proceeds when the heating up temperature reaches 373 K, a sudden and sharp increase of the total concentration was observed around 373 K, as shown in Figure 10b. Such observations could also be a clue for detecting the proceeding of the reaction during the cooling down stage at a certain reaction temperature.

Based on the above discussion, it could be possible now to follow the kinetics of fast reactions that take place under the sub-critical condition using the mathematical model and the strategy developed in this work. The most important conclusion obtained in this study is that in the case of a fast reaction (as defined in the introduction section), all the reaction stages should be taken into consideration during investigating the kinetics of such reactions (that is, heat up, transferring, and cooling down). However, the effect of each reaction stage on the overall reaction kinetics differs based on the chemistry of the reaction itself. Moreover, it is not possible to get a critical time, below which the results are significantly misinterpreted by assuming the reactor to be at the reaction temperature for only the time in which the reactor is in the salt bath. Since such critical time varies from one particular reaction to another, it could only be obtained by using the present model to study the effect of each stage on the overall reaction kinetics and finding out such critical time by comparing the actual experimental results with those obtained theoretically.

Future Work

In the very near future we are going to present the experimental data for the kinetic study of the synthesis of a protein-based biodegradable plastic prepared from the bovine serum albumin in a batch reactor, which has been synthesized in our previous work[23] (as described in the introduction section). Such results could be used to show the validity of the present strategy and kinetic model.

Acknowledgments

Part of this research was funded by the Ministry of Education, Culture, Sports, Science and Technology of Japan in the form of the 21st century COE Program (E-1), entitled "Science and Engineering for Water-Assisted Evolution of Valuable Resources and Energy from Organic Wastes."

Literature Cited

1. Krammer P, Vogel H. Hydrolysis of ester in subcritical and supercritical Water. *Supercrit Fluids.* 2000;16:189-206.
2. Tromp RH, Postorino P, Neilson GW Ricci MA, Soper AK. Neutron diffraction studies of H2O/D2O at supercritical temperatures: a direct determination of gHH(r), gOH(r) and gOO(r). *Chem Phys.* 1994;101: 6210-6214.
3. Ohtaki H, Radnai T, Yamaguchi T. Structure of water under the subcritical and supercritical conditions studied by means of solution x-ray diffraction. *Chem Soci Rev.* 1997;41-51.
4. Deshpande GV, G D Holder, Bishop AA, Gopal J, Wender I. Extraction of coal using supercritical water. *Fuel.* 1984;63:956-960.
5. Kershaw JR. Supercritical fluids in coal processing. *Environ Sci Technol.* 1993;27:806-809.
6. Daimon H, Kang K, Sato N, Fuje K. Development of marine waste recycling technologies using sub- and supercritical water. *Chem Eng Japan.* 2001;34:1091-1096.
7. Modell M. *Standard Handbook of Hazardous Waste Treatment and Disposal*, Freeman HM (ed.), Sec. 8.11. New York: McGraw Hill; 1989.
8. Goto M, Nada T, Kodama A, Hirose T. Kinetic analysis for destruction

of municipal sewage sludge and alcohol distillery wastewater by sub-critical water oxidation. *Ind Eng Chem Res.* 1999;38:1863-1865.
9. Yoshida H, Terashima M, Takahashi Y. Production of organic acids and amino acids from fish meat by subcritical water hydrolysis. *Biotechnol Prog*. 1999;15:1090-1094.
10. Yoshida H, Atarashi M, Shigeta T. Conversion of entrails of fish waste to valuable resources by sub-critical water hydrolysis. Proceedings of Joint six International Symposium on Hydrothermal Reactions (ISHR-6) and Fourth International Conference on Solvothermal Reactions (ICSTR-4). July 2000, Kochi, Japan, 122-125.
11. Yoshida H, Takahashi Y, Terashima M. A simplified reaction model for production of oil, amino acids and organic acids from fish meat by hydrolysis under sub-critical and supercritical conditions. *J Chem Eng Japan.* 2003;36(4):441-448.
12. Yoshida H, Tavakoli O. Sub-critical water hydrolysis treatment of squid waste entrails and production of organic acid, amino acid, and fatty acids. *J Chem Eng Japan.* 2004;37(2):253-260.
13. Yoshida H, Nakahashi T. Production of useful substances from meat and bone meal by sub-critical water hydrolysis. Proceedings of the 10th APCChE Congress. Kitakyashu, Japan, 2004;A272.
14. Tavakoli O, Yoshida H. Effective recovery of harmful metal ions from squid wastes using subcritical and supercritical water treatment. *Environ Sci Technol.* 2005;39(7):2357-2363.
15. Yoshida H, Katayama Y. Production of useful substances from wood wastes by sub-critical water hydrolysis. Proceedings of the 10th APCChE Congress. Kitakyashu, Japan, 2004;A272.
16. Abdelmoez W, Yoshida H. An overview of the applications of the subcritical water hydrolysis technology in waste reuse, recycle, and treatment. Proceedings of El-Minia International Conference, Towards a Safe and Clean Environment, TSCE'05, El-Minia, Egypt, 15-17 April, 2005. E3–4.
17. Antal MJ, Allen SG, Schulman D, Xiaodong Xu. Biomass gasification in supercritical water. *Ind Eng Res*. 2000;39:4040-4053.
18. Kabyemela BM, Adschiri T, Malaluan RM, Arai K. Kinetics of glucose epimerization and decomposition in subcritical and supercritical water. *Ind Eng Chem Res.* 1997;36(5):1552-1558.
19. Kabyemela BM, Adschiri T, Malaluan RM, Arai K. Degradation kinetics of dihydroxyacetone and glyceraldehyde in subcritical and supercritical water. *Ind Eng Chem Res.* 1997;36:2025-2030.
20. M. Sasaki, Fang Z, Fukushima Y, Adschiri T, Arai K. Dissolution and hydrolysis of cellulose in subcritical and supercritical water. *Ind Eng Res.* 2000;39:2883-2890.
21. Sakaki T, Shibata M, Sumi T, Yasuda S. Saccharifaction of cellulose using a hot-compressed water-flow reactor. *Ind Eng Res.* 2002;41:661-665.
22. Nagamori M, Funazukuri T. Glucose production by hydrolysis of starch under hydrothermal conditions. *J Chem Tech Biotec.* 2004;79:229-233.
23. Abdelmoez W, Yoshida H. Synthesis of a novel protein-based plastic using sub-critical water technology. *AIChE J.* 2006;52:2607-2616.
24. Jacobsen SE, Wyman EC. Heat transfer considerations in design of a batch tube reactor for biomass hydrolysis. *Appl Bioch Biotech*. 2001;91–93:377-386.
25. Discover the origins of some of the world's most consistently pure products, "synthetic Glycerin products." The Dow Chemical Company free report, Form No. 115–00645-1199X SMG.

Manuscript received Dec. 20, 2005, and revision received July 17, 2006.